Structures of Michaelis and Product Complexes of Plant Cytokinin Dehydrogenase

Malito, Enrico; Coda, Alessandro; Bilyeu, Kristin D.; Fraaije, Marco; Mattevi, Andrea

Published in:
Journal of Molecular Biology

DOI:
10.1016/j.jmb.2004.06.083

Publication date:
2004

doi:10.1016/j.jmb.2004.06.083 J. Mol. Biol. (2004) 341, 1237–1249

JMB

Available online at www.sciencedirect.com

SCIENCE DIRECT®

ELSEVIER

Structures of Michaelis and Product Complexes of Plant Cytokinin Dehydrogenase: Implications for Flavoenzyme Catalysis

Enrico Malito[1], Alessandro Coda[1], Kristin D. Bilyeu[2], Marco W. Fraaije[3] and Andrea Mattevi[1]*

[1]*Department of Genetics and Microbiology, University of Pavia, Via Ferrata 1, 27100 Pavia, Italy*

[2]*USDA/ARS, 210 Waters Hall University of Missouri Columbia, MO 65211, USA*

[3]*Laboratory of Biochemistry University of Groningen Nijenborgh 4, 9747 AG Groningen, The Netherlands*

**Corresponding author*

Cytokinins form a diverse class of compounds that are essential for plant growth. Cytokinin dehydrogenase has a major role in the control of the levels of these plant hormones by catalysing their irreversible oxidation. The crystal structure of *Zea mays* cytokinin dehydrogenase displays the same two-domain topology of the flavoenzymes of the vanillyl-alcohol oxidase family but its active site cannot be related to that of any other family member. The X-ray analysis reveals a bipartite architecture of the catalytic centre, which consists of a funnel-shaped region on the protein surface and an internal cavity lined by the flavin ring. A pore with diameter of about 4 Å connects the two active-site regions. Snapshots of two critical steps along the reaction cycle were obtained through the structural analysis of the complexes with a slowly reacting substrate and the reaction product, which correspond to the states immediately before (Michaelis complex) and after (product complex) oxidation has taken place. The substrate displays a "plug-into-socket" binding mode that seals the catalytic site and precisely positions the carbon atom undergoing oxidation in close contact with the reactive locus of the flavin. A polarising H-bond between the substrate amine group and an Asp-Glu pair may facilitate oxidation. Substrate to product conversion results in small atomic movements, which lead to a planar conformation of the reaction product allowing double-bond conjugation. These features in the mechanism of amine recognition and oxidation differ from those observed in other flavin-dependent amine oxidases.

Keywords: flavoenzyme; mechanism of catalysis; cytokinin; crystallography

Introduction

Cytokinins are a class of plant hormones that promote cell division and differentiation.[1] These compounds are derivatives of adenine and are classified on the basis of the variable substituent at the adenine C6 position (Figure 1). The most predominant cytokinins have an unsaturated isoprenoid side-chain; examples are *trans*-zeatin and N^6-isopentenyladenine (Figure 1). Some physiologically active cytokinins have an aromatic side-chain, the best known example being N^6-benzyladenine.

Cytokinins are essential for plant morphogenesis, especially in the formation of roots and shoots. Their mechanisms of action at both the molecular and cellular levels are still far from being fully understood. Recent studies have revealed that cytokinins exert their function primarily through the regulation of the cell-cycle.[2,3] Considerable efforts in the last years have been directed towards the discovery of proteins and enzymes that function in cytokinin signalling and metabolism.[4,5] Cytokinin dehydrogenase (CKX) has been found to play a major role in cytokinin catabolism.[6] The physiological function of this enzyme has been investigated extensively through engineering of tobacco transgenic plants overexpressing *Arabidopsis thaliana* CKX.[2,3] Increased enzyme activity causes drastic

Abbreviations used: CKX, cytokinin dehydrogenase (EC 1.5.99.12); rmsd, root-mean-square deviation; PEG5000 MME, polyethyleneglycol 5000 monomethylether.

E-mail address of the corresponding author: mattevi@ipvgen.unipv.it

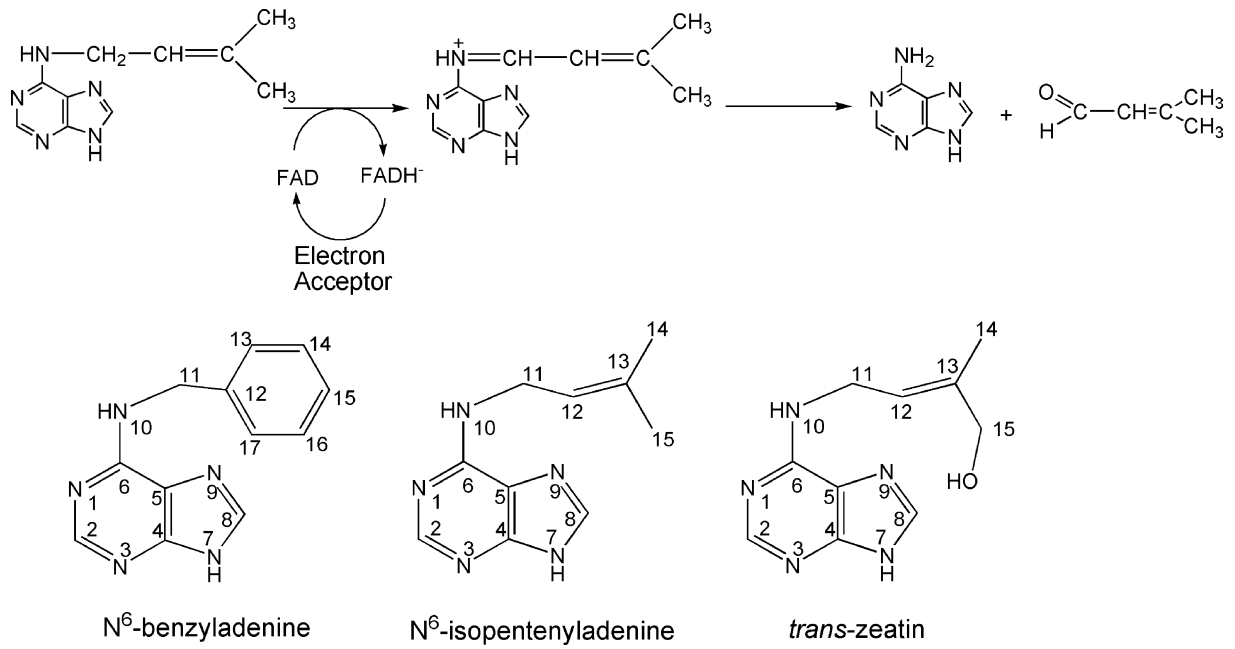

Figure 1. Top: Scheme of the reaction catalysed by CKX with reference to the N^6-isopentenyladenine substrate. Bottom: Chemical formula and atomic numbering for the ligands used in the crystallographic studies. This numbering has been used also for the atomic coordinates deposited with the Protein Data Bank.

abnormalities in the growth and development of the CKX overexpressing plants, highlighting the fundamental role of CKX in the control of cytokinin levels. Sequence and biochemical analysis has shown that CKX is a flavoenzyme that belongs to a class of oxidoreductases that encompasses oxidases and dehydrogenases containing a covalent or non-covalent FAD cofactor.[6,7] The enzyme catalyses the irreversible degradation of cytokinins through the oxidation of the secondary amine group on the side-chain of the adenine ring (Figure 1).[8] The resulting imine product is subsequently hydrolysed, producing adenine and an aldehyde molecule, this step being most likely non-enzymatic,[9,10] as observed in other flavin-dependent amine oxidases. Therefore, CKX belongs to the class of flavin-dependent amine oxidases/dehydrogenases.

Genes encoding for CKX have been found in many plants.[6] In biochemical terms, the most thoroughly studied CKX is the enzyme from *Zea mays*.[9,10] This 57 kDa monomeric protein is most active against cytokinins that have an isoprenoid substituent, including *trans*-zeatin and N^6-isopentenyladenine (Figure 1). Instead, it exhibits little or no activity against molecules bearing an aromatic side-chain. CKX was classified initially as an oxidase because molecular oxygen was thought to be the electron acceptor required for regeneration of the oxidised flavin during turnover. However, recent kinetic data on the wheat enzyme show that oxygen is a poor substrate.[8] Other compounds, such as certain quinones,[10] are more efficient electron acceptors and are likely to be the physiological substrates. Because of this, the enzyme is now classified as a dehydrogenase. Consistent with the recent literature, we prefer to maintain the widely used CKX acronym to identify the enzyme.

Here, we describe the crystal structure of recombinant *Zea mays* CKX in the native state and in complex with reaction products and a slowly reacting substrate (Figure 1). The X-ray analysis unravels the molecular basis for the specific recognition of the "isoprenoid" cytokinins and for the mechanism of catalysis.

Results

Overall structure

The crystal structure of recombinant native CKX was solved by single isomorphous replacement and refined to 1.7 Å resolution. The complexes with *trans*-zeatin, N^6-isopentenyladenine and N^6-benzyladenine (Figure 1) were solved by difference Fourier methods and refined to 1.9–2.0 Å resolution (Table 1). The CKX crystals are remarkably well ordered, resulting in electron density maps of excellent quality (Figure 2). The refined structures (Table 2) exhibit good stereochemical parameters with no residue in the disallowed regions of the Ramachandran plot. The N-terminal 40 amino acid residues are not visible in the electron density map, in agreement with the observation that CKX is produced as a precursor protein undergoing an N-terminal cleavage upon processing.[11] CKX is known to be a glycosylated enzyme,[11] although the composition and size of the glycosidic chains have not been investigated in detail. The electron density now shows clearly that there are four glycosylation sites. It was possible to model a total

Table 1. Data collection statistics

			Ligand		
	Native	Hg derivative	Isopentenyl-adenine	Benzyladenine	*trans*-Zeatin
Space group	$P4_22_12$	$P4_22_12$	$P4_22_12$	$P4_22_12$	$P4_22_12$
Unit cell dimensions					
a (Å)	171.69	170.54	171.35	168.68	171.03
b (Å)	171.69	170.54	171.35	168.68	171.03
c (Å)	54.32	53.93	54.17	53.75	54.14
Resolution (Å)[a]	1.7 (1.79–1.70)	3.0 (3.15–3.00)	1.9 (2.00–1.90)	2.0 (2.11–2.0)	1.9 (2.00–1.90)
R_{sym}[a,b]	0.083 (0.338)	0.163 (0.304)	0.099 (0.398)	0.126 (0.40)	0.105 (0.463)
Completeness[a] (%)	98.8 (97.9)	98.9 (97.7)	99.6 (99.1)	99.2 (97.1)	98.9 (97.9)
$I/\sigma(I)$[a]	14.6 (4.4)	9.5 (3.4)	13.4 (2.9)	11.6 (2.4)	11.2 (2.7)
Unique reflections	88,469	16,551	64,030	52,429	63,311
Redundancy	4.9	3.4	4.5	5.0	4.4
R_{deriv}[c]	–	0.18	–	–	–
R_{cullis}[d]	–	0.86	–	–	–
Phasing power (centric/acentric)	–	0.73/0.86	–	–	–

[a] Data for the highest-resolution shell are given in parentheses.
[b] $R_{sym} = \sum_h \sum_i |I_i(hkl) - \langle I(hkl)\rangle| / \sum_h \sum_i I(hkl)$.
[c] $R_{deriv} = \sum ||F_{PH}| - |F_P|| / \sum |F_P|$, where F_{PH} is the structure factor for the derivative and F_P is the structure factor for the native crystal.
[d] $R_{cullis} = \sum ||F_{PH} \pm F_P| - F_H| / \sum |F_{PH} \pm F_P|$, where F_{PH} and F_P are defined as above, and F_H is the calculated heavy-atom structure factor. Centric reflections only were included in the calculation.

of five ordered sugar residues, one residue each bound to Asn63, Asn89, and Asn294, and a two residue chain linked to Asn134. The ordered sugar molecules were modelled tentatively as *N*-acetyl-D-glucosamine, this interpretation being based solely on the fitting to the electron density.

CKX exhibits the same two-domain topology of the members of the vanillyl-alcohol oxidase family of flavoenzymes (Figure 3).[7] The FAD-binding domain comprises residues 40–244 and 492–534, whereas the substrate-binding domain consists of residues 245–491. A search of the Protein Data Bank with the program DALI[12] shows that the closest homologue of CKX is cholesterol oxidase from *Brevibacterium sterolicum* (PDB entry 1I19) with a root-mean-square deviation (rmsd) of 3.8 Å for 392 equivalent C^α atoms and 14% sequence identity.[13] Comparison of the protein structures reveals a similar folding topology with a large deviation in residues 344–396 of CKX. This segment comprises two α-helices that are part of the active site and adopts a different conformation with respect to the corresponding residues of cholesterol oxidase (347–431). This feature highlights the notion that the members of this oxidoreductase family share a similar folding topology and FAD-binding site but are highly diverse in the architecture of their catalytic centre.[7]

The FAD-binding site

The cofactor is bound covalently to the protein.[9] The site of attachment is the ND1 atom of His105, which binds to the 8-methyl group of the flavin ring

Table 2. Refinement statistics

		Ligand		
	Native	Isopentenyl-adenine	Benzyladenine	*trans*-Zeatin
Resolution range (Å)	15.0–1.7	15.0–1.9	15.0–2.0	15.0–1.9
R-factor (R_{free})[a]	0.198 (0.214)	0.205 (0.221)	0.198 (0.218)	0.206 (0.223)
No. non-H protein atoms[b]	4421	4096	4095	4117
No. water molecules	626	287	284	290
No. FAD atoms	53	53	53	53
No. ligand atoms	–	15	16	16
rmsd values				
Bond length[c] (Å)	0.006	0.007	0.005	0.006
Bond angle[c] (deg.)	0.9	1.0	1.0	1.1
Ramachandran plot[d]				
Most favourable region (%)	91.2	91.4	90.5	90.7
Disallowed regions (%)	0.00	0.00	0.00	0.00

[a] $R_{factor} = \sum ||F_{obs}| - |F_{calc}|| / \sum |F_{obs}|$. R_{free} is the R_{factor} value for 5% of the reflections excluded from the refinement.
[b] CKX is glycosylated at four sites. The final models contain five sugar residues.
[c] Root-mean-square deviations (rmsd) from ideal values calculated with Refmac.[28]
[d] Figures from PROCHECK.[30]

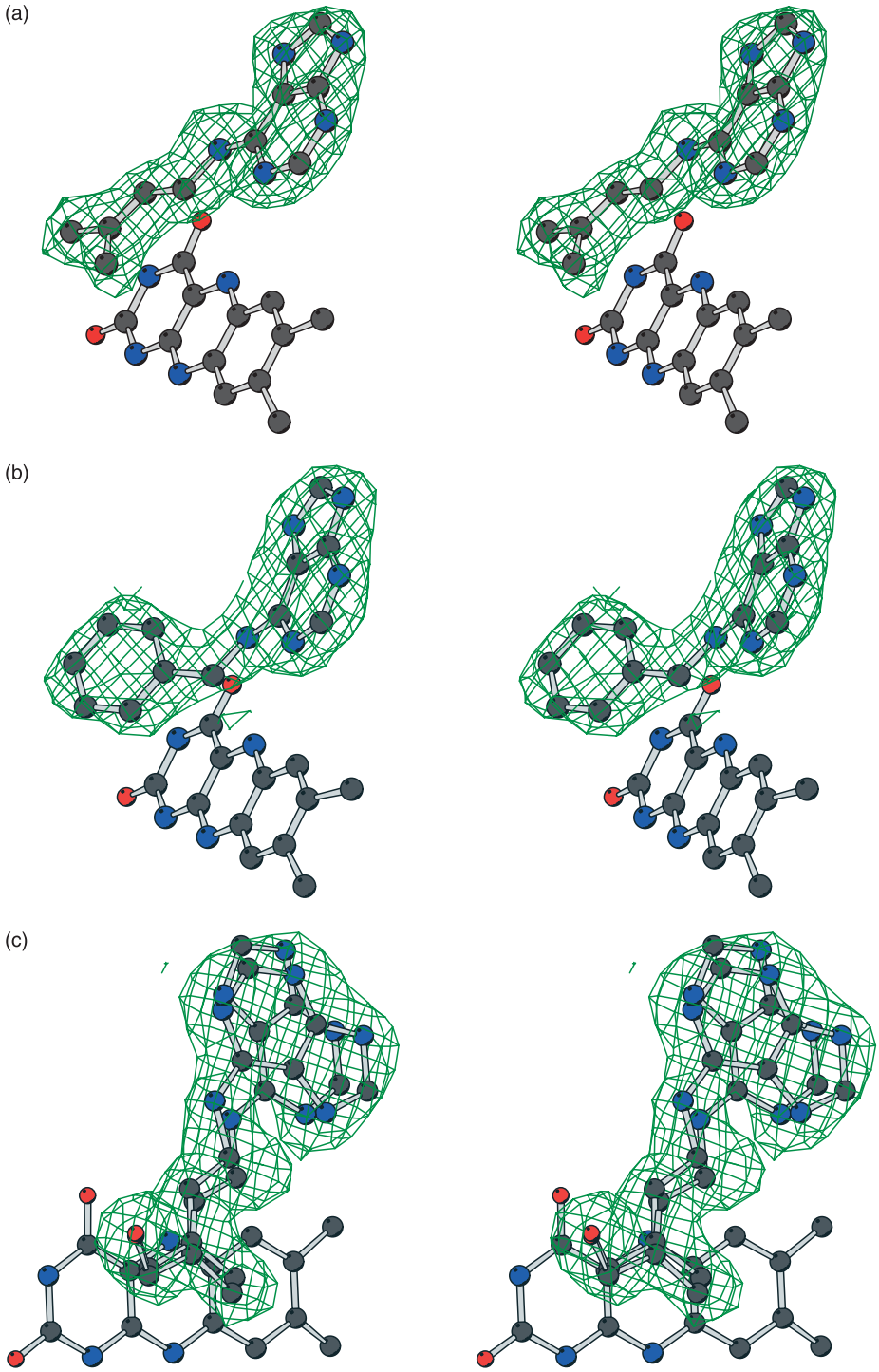

Figure 2. Unbiased $2F_o - F_c$ electron density maps observed in the active sites of the complexes obtained by soaking in (a) N^6-isopentenyladenine, (b) N^6-benzyladenine, and (c) *trans*-zeatin. The electron density of *trans*-zeatin is less well resolved than that obtained from the N^6-isopentenyladenine soaking, indicating disorder or multiple conformations. A tentative interpretation is that the adenine ring of *trans*-zeatin adopts two alternative conformations. The contour level is 1σ. The maps were calculated before the ligand atoms were included in the refinement. Carbon atoms are in black, oxygen atoms are in red, and nitrogen atoms are in blue.

(Figure 4). The covalent flavinylation site does not show any unusual or strained conformation like that found in the flavinylated cysteine residue of human monoamine oxidase.[14] The covalent linkage is expected to be one of the main factors that determine the relatively high (8 mV) redox potential of CKX.[10,15]

The ADP-ribityl segment of the prosthetic group is embedded in the FAD domain, and is completely solvent-inaccessible (Figure 3). There are

Figure 3. Overall structure of maize CKX monomer. The FAD-binding domain (residues 40–244 and 492–534) is shown in blue and the substrate-binding domain (residues 245–491) is shown in red. The FAD and the oxidised N^6-isopentenyladenine ligand are shown, respectively, in yellow and black ball-and-stick representation. The N-terminal and C-terminal residues are labelled by N and C, respectively.

several H-bond interactions that involve main-chain and side-chain protein atoms as well as ordered solvent molecules (Figure 4). The negative charge of the pyrophosphate moiety is compensated for by the interactions with a constellation of backbone nitrogen atoms of Gly102, Arg103, Gly104, His105, Ser106 and Thr174. The isoalloxazine ring adopts a planar conformation. It is located at the bottom of an ellipsoidal cavity, which, in the native structure, is occupied by at least seven ordered water molecules, one of them being H-bonded to the flavin N5 atom (Figure 4). The cavity is connected to the outside through a narrow pore (Figure 5(a) and (b)), whose entrance is lined by Asp169, Trp397 and Leu458. With a total volume of about 400 Å^3, the cavity is able to bind the reactive part of the substrate (Figure 1), thus forming the catalytic site, as described in the next section.

Soaking in N^6-isopentenyladenine: complex between reduced enzyme and reaction product

The crystals grow in conditions of low pH (pH 4.6). Kinetic analysis (unpublished data) shows that the enzyme is catalytically active also at this low pH value, the only significant change in the kinetic parameters being a 30% reduction in the k_{cat} with respect to the value measured at the optimal pH (pH 8). N^6-Isopentenyladenine is one of the best substrates of maize CKX, displaying a k_{cat} of $\sim$150 s^{-1} and a K_M of 40 μM when using an effective electron acceptor (Figure 1).[10] Soaking of the crystals in a solution containing this compound led to a rapid bleaching of the yellow colour, characteristic of the oxidised flavin. This indicates that the crystalline enzyme reacts with the substrate, resulting in the accumulation of the reduced form of the cofactor although it cannot be ruled out that a fraction of the FAD molecules are in the oxidised or semireduced forms. Such stabilisation of the reduced enzyme during aerobic soaking reflects the slow reactivity of CKX towards oxygen.[8,10] The 1.9 Å resolution map calculated from a soaked crystal reveals a strong electron density peak in front of the flavin ring (Figure 2(a)), extending from the cavity through the pore to the protein surface (Figure 5(a) and (b)). A molecule of the product resulting from the oxidation of N^6-isopentenyladenine (Figure 1) perfectly fits the electron density (Figure 2(a)). In particular, the map has a flat shape consistent with the presence of a bound imine product molecule, which is expected to be planar because of the conjugation of its double bonds (Figure 1). Trapping of the reaction product reflects the fact that the crystal environment probably makes product release rate-limiting in the reaction catalysed by the crystalline enzyme. Therefore, the excess of substrate employed for soaking leads to the accumulation of the reduced enzyme–product complex.

Ligand binding does not cause any significant conformational change. The rms deviation between the native and the ligand-bound structures is only 0.13 Å for all C^α atoms. Also, the active site is essentially indistinguishable from that of the native structure; ligand binding simply occurs through the displacement of six ordered water molecules and no other modifications. In this regard, it is noteworthy that even the active site water molecules that are in van der Waals and H-bond contact with the ligand atoms (Figure 6(a) and (b)) occupy positions equivalent to those of ordered water molecules present in the native structure. The virtually exact similarity between the structures of the oxidised native enzyme and the reduced enzyme product complex indicates that cofactor reduction is not associated with conformational changes in the residues surrounding the active site.

The imine form of N^6-isopentenyladenine binds with the isopentenyl side-chain inside the cavity, while the adenine ring is exposed on the protein surface (Figure 5). This binding mode positions the reactive N10–C11 (Figure 1) atoms at the orifice of the internal cavity (Figure 5(a)) so that the ligand acts like a plug that seals the pore connecting the cavity to the surface. As a result, the isopentenyl moiety is made fully solvent-inaccessible, lying above and in van der Waals contact (about 4 Å) with the flavin ring (Figure 6(a)). The adenine group binds in a funnel-shaped site on the protein surface (Figure 5(b)); it is sandwiched between the side-chains of Val378 and Pro427 (Figure 6(a)) with its edge exposed to solvent (Figure 5(b)). Except for N1, all the nitrogen atoms of the ligand are engaged in H-bond interactions (Figure 6(a) and (b)) either

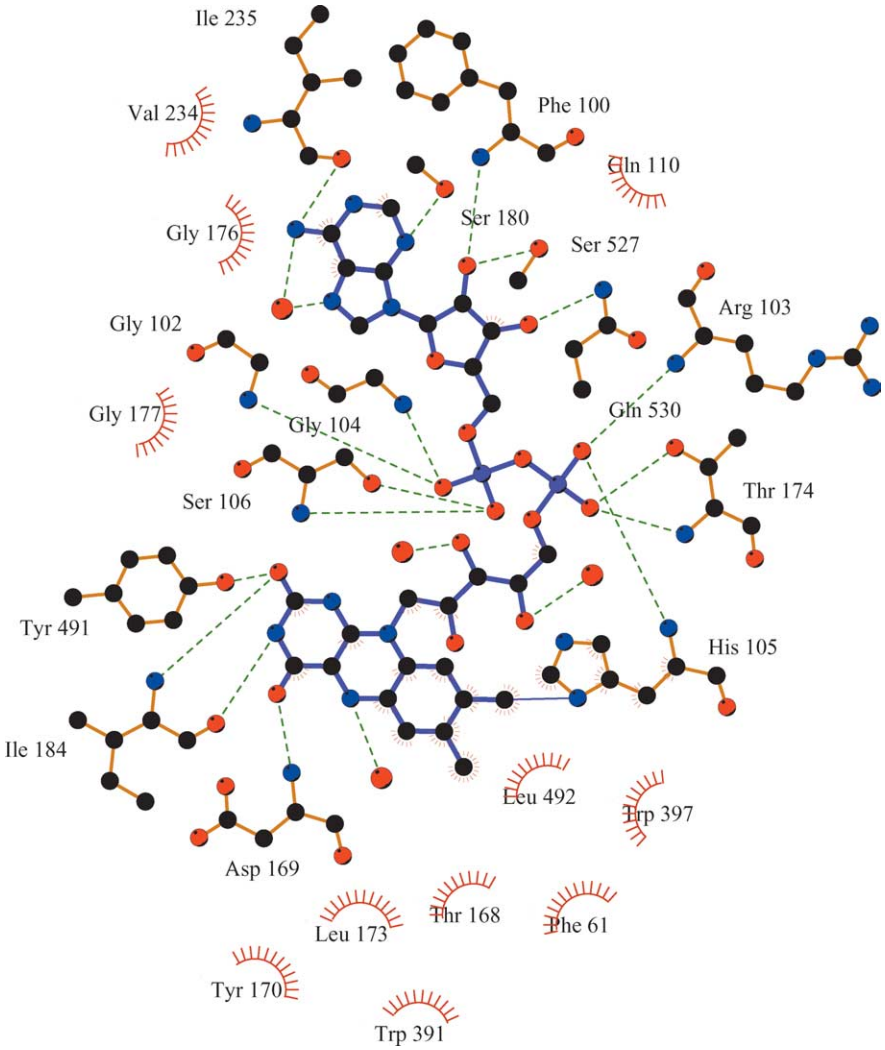

Figure 4. Ligplot[35] drawing showing the interactions of FAD with CKX. Atom colours are as in Figure 2. Broken lines indicate all potential H-bonds. "Radiating" spheres indicate hydrophobic contacts between carbon atoms of the cofactor and the neighbouring residues.

with solvent molecules (N9 and N3) or protein side-chains (N10 to Asp169, N7 to Glu381). The H-bonding Asp169 residue is strongly conserved among the known CKX sequences,[6] and appears to play a central role. In addition to the H-bond with the ligand N10 atom, the carboxylate group of this amino acid is within H-bond distance from a side-chain oxygen atom of Glu288 (Figure 6). The presence of such carboxylate–carboxylate pair between Asp169 and Glu288 implies that one of two side-chains is protonated to allow formation of a H-bond interaction (Figure 6(b)).

N^6-Benzyladenine binding

N^6-Benzyladenine (Figure 1) is a poor substrate of CKX,[10] with a turnover number of 0.2 s^{-1}. Soaking in a solution containing this compound does not alter the crystal colour, even after prolonged exposure, indicating that no changes in the crystalline enzyme redox state take place. The electron density map calculated at 2.0 Å resolution (Figure 2(b)) reveals a peak, which is juxtaposed to the flavin and can be explained by the binding of a substrate molecule to the enzyme. Most importantly, the density has a "curved" non-planar appearance consistent with the tetrahedral configuration of the C11 atom of the substrate (Figures 1 and 2(b)). All attempts to model the ligand as the imine reaction product were always unsatisfactory and when subjected to the least-squares refinement, the atoms were "pushed" towards a non-planar conformation. Taken together, these observations clearly indicate that soaking with the slowly reacting N^6-benzyladenine leads to the formation of the complex between the oxidised protein and the substrate (Michaelis complex).

Binding of N^6-benzyladenine is similar to but not identical with that of the imine form of N^6-isopentenyladenine (Figures 2(b) and 7). The benzyl ring occupies the internal cavity,

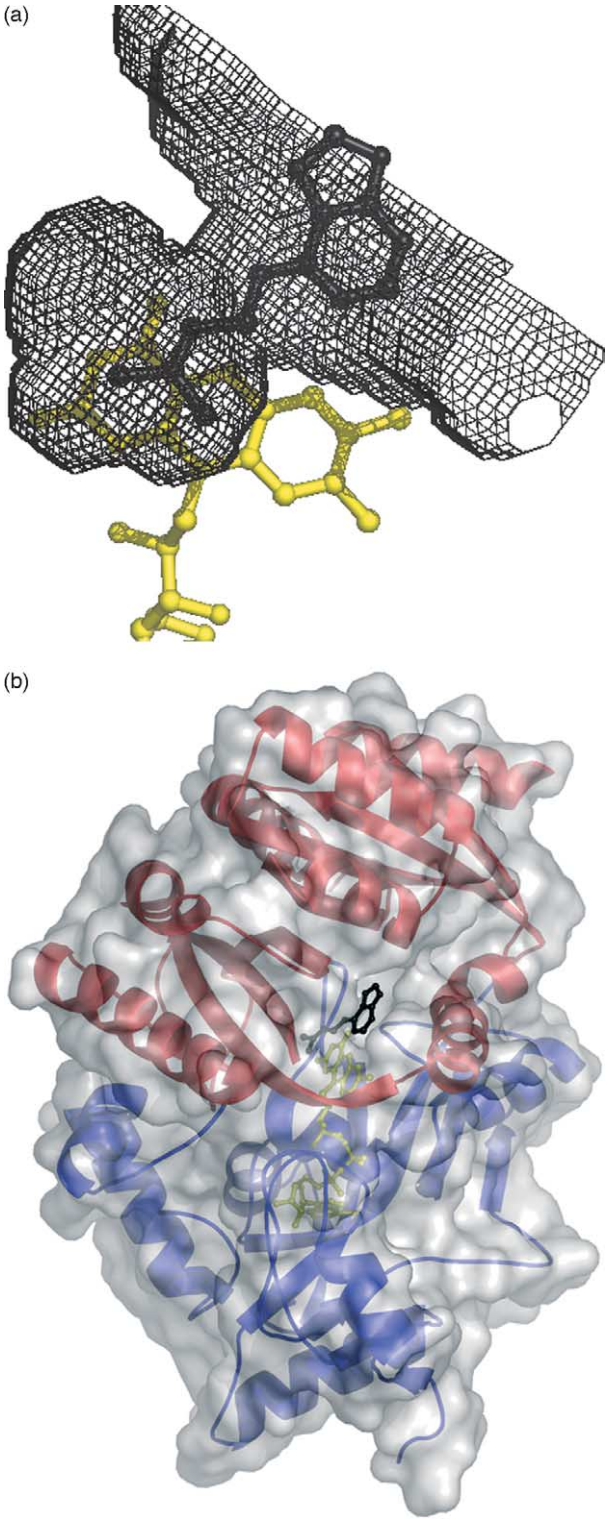

Figure 5. Shape and architecture of the active site of CKX. (a) Close-up view of the protein surface in the region surrounding the active site in approximately the same orientation as in Figure 3. The picture outlines the internal cavity located in front of the flavin ring (yellow) connected through a pore to the outside surface. The oxidised N^6-isopentenyladenine ligand is shown in black. The cavity and surface calculations were done using a probe radius of 1.4 Å.[31] (b) View of the CKX monomer surface. The isopentenyl substituent is buried inside the internal cavity, whereas the adenine ring sticks out on the surface with its edge accessible to the solvent. For reference, the C^α trace is shown in ribbon representation with the same colouring scheme as that in Figure 3.

establishing van der Waals contacts with the protein and flavin atoms. The N10–C11 atoms bind at the cavity pore, being engaged in a H-bond between N10 and the side-chain of Asp169. The adenine ring sits outside the cavity, with a slightly tilted orientation (11°) with respect to that seen in the N^6-isopentenyladenine structure. This small reorientation reflects the tetrahedral configuration of the N10–C11 atoms on the adenine substituent.

With respect to the implications for catalysis, it is of interest to analyse the stereochemistry of the ligand–flavin interactions (Figure 7). The flavin N5 and the substrate C11 atoms, which are at only 2.7 Å distance from each other, establish the closest contact. This distance is shorter than the corresponding one (3.3 Å) found in the N^6-isopentenyladenine imine complex, reflecting the non-planar conformation of the N10–C11 moiety of N^6-benzyladenine, which brings the C11 atom in close contact with the flavin. A point with far-reaching implications for catalysis is that the substrate N10 and the flavin ring (Figures 2(b) and 7) are opposite to each other with respect to the line connecting the substrate C11 to the flavin N5 atoms. Consequently, the ligand amine group is at a distance of no less than 4.5 Å from the flavin ring.

Similar to the N^6-isopentenyladenine imine complex structure, the complex with N^6-benzyladenine shows no conformational change with respect to the native structure with rmsd of 0.23 Å for the C^α atoms. The only noticeable variation affects Glu381 in the adenine site (Figure 6). This residue lacks clear electron density, suggesting that in the N^6-benzyladenine complex it probably adopts multiple conformations.

Complex with *trans*-zeatin

We performed a binding study using *trans*-zeatin, which is a good substrate of CKX and differs from N^6-isopentenyladenine by just one additional terminal OH group on the isopentenyl side-chain (Figure 1). Soaking resulted in a fast disappearance of the yellow colour, indicative of flavin reduction. The electron density map indicates clearly the presence of the bound reaction product with a planar N10–C11 imine bond (Figure 2(c)). However, the electron density in the region of the adenine ring is somewhat broader and less resolved than that observed for the N^6-isopentenyladenine soaking. Refinement calculations and inspection of the difference Fourier maps led to the tentative interpretation that the oxidised *trans*-zeatin might bind in two alternative conformations. The first one is identical with that found in the N^6-isopentenyladenine complex, whereas in the second conformation, the adenine ring is flipped by 180°. Such a

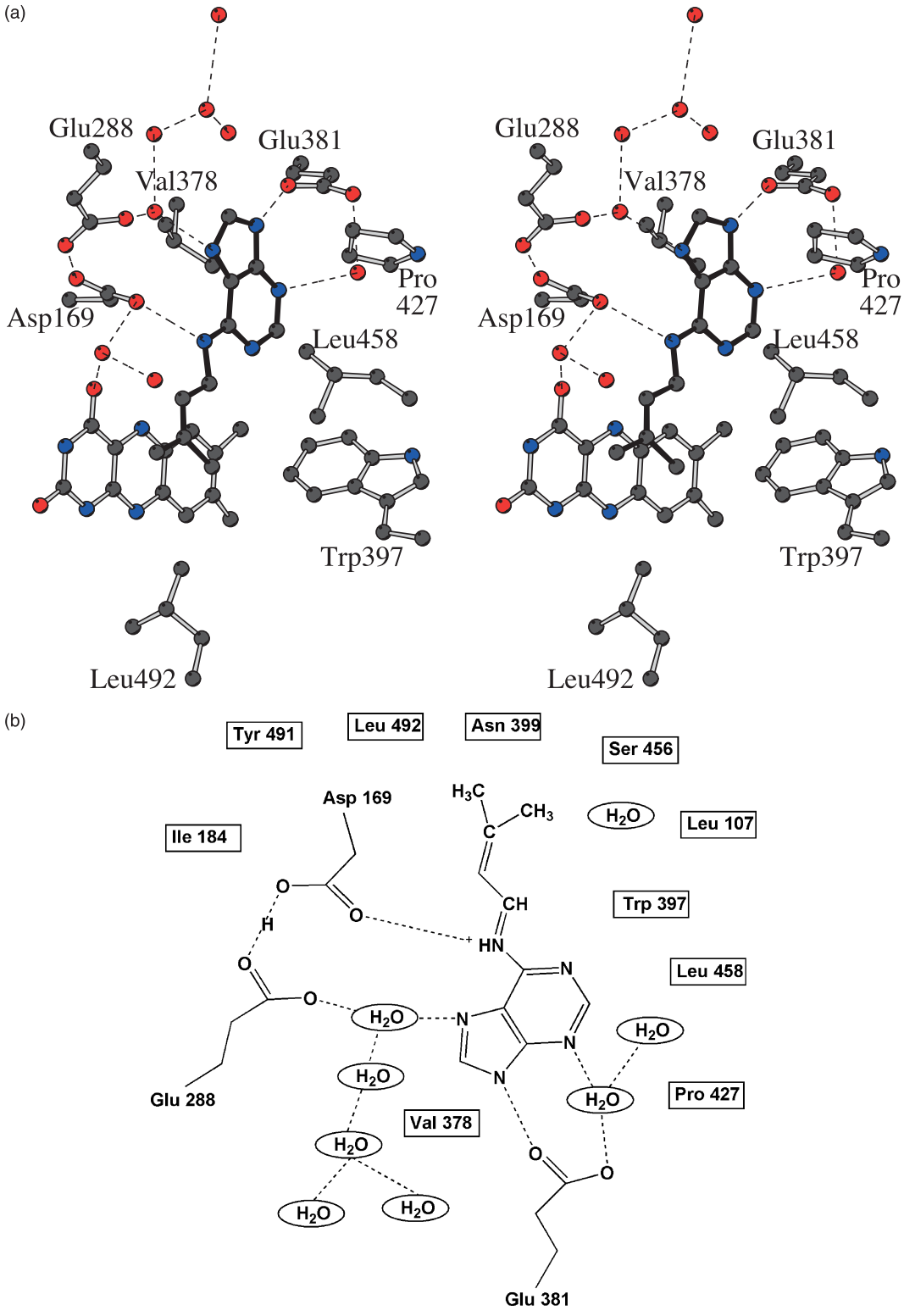

Figure 6. (a) Stereo view of the active site with the oxidised N^6-isopentenyladenine imine product bound. With respect to Figure 3, the protein has been rotated by about 60° on the vertical axis in the plane of the paper. H-bonds are shown as broken lines. Ordered water molecules are depicted as spheres. Atom colours are as in Figure 2. (b) Schematic representation of the oxidised N^6-isopentenyladenine binding site. Glu288 and Asp169 form a carboxylate–carboxylate pair, which is expected to share a proton to allow formation of a H-bond interaction.

ring flipping allows all polar atoms to be engaged in H-bond interactions and does not affect the pentenyl adenine side-chain, which binds in the same conformation and position in the two conformers. Therefore, the presence of multiple conformations of the adenine ring does not alter the binding of the reactive part of the ligand located in front of the flavin.

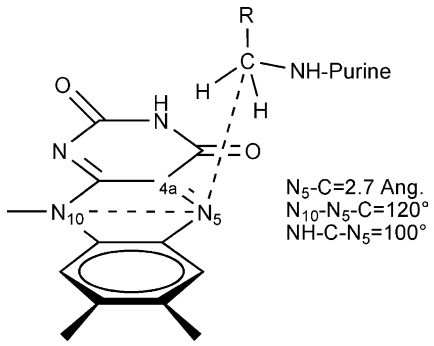

Figure 7. Stereochemistry of the interactions between the flavin ring and the reactive N10–C11 amino group (Figure 1) of the substrate with reference to the N^6-benzyladenine complex.

Discussion

Substrate binding

Maize CKX exhibits the characteristic two-domain folding topology of the oxidoreductases of the vanillyl oxidase family (Figure 3) but its active site cannot be related to that of any other family member of known three-dimensional structure. CKX is active on several cytokinins,[6,8] a class of plant hormones derived from adenine. From a chemical standpoint, these compounds consist of two building blocks, the adenine ring and the C6-bound aliphatic side-chain that represents the site of enzymatic oxidative attack (Figure 1). This structure is matched by the bipartite architecture of the CKX active site, which consists of two entities: an internal cavity lined by the flavin ring; and a funnel-shaped region on the protein surface. These two regions form the binding site for the aliphatic side-chain of the substrate and the adenine ring, respectively (Figure 5(a)). A pore of diameter of about 4 Å connects the two sub-sites.

The bipartite nature of the CKX active site is instrumental to a sort of plug-into-socket substrate-binding mode. The adenine is recognised by a set of aliphatic side-chains and Glu381, which binds to the N3 and N7 atoms of the ring. The edge of the ring is oriented towards the solvent and is exposed on the protein surface (Figure 5(b)). This binding mode explains the fact that CKX is able to oxidise N^6-isopentenyladenosine with a similar kinetic efficiency when compared with N^6-isopentenyl-adenine.[9,10] It is conceivable that the ribose group of this substrate will stick out into the solvent without greatly hampering binding and catalytic activity. The reactive group of the cytokinin substrates extends snugly from the adenine site through the pore into the internal cavity, where it is effectively made solvent-inaccessible. Thus, a solvent-protected environment is created for the reaction to occur, using the adenine ring as a seal for the catalytic site (Figure 5(a)). Substrate binding does not involve domain or loop movements, which are often employed by dehydrogenases and oxidases to shield the substrate from the solvent.[16] On the contrary, the active site of CKX displays a remarkable degree of pre-organisation and complementarity with respect to the cytokinin substrates. This pre-organisation concerns the protein conformation and a constellation of substrate-binding water molecules that are present in both the native and ligand-bound enzyme (Figure 6(a)).

In such a pre-organised binding site, a key element is the Asp169-Glu288 pair. One of the carboxylate oxygen atoms of Asp169 is H-bonded to the ligand N10 atom in all structures investigated (both product and Michaelis complexes) acting as key element for recognition of the substrate amine group (Figure 6(b)). The other carboxylate oxygen atom of Asp169 is engaged in a H-bond with Glu288. The interaction between these two side-chains might be favoured by the acidic pH of the crystallisation medium. However, as indicated by the soaking experiments, the crystalline enzyme is active, indicating that the crystal structure conformation is catalytically competent. The presence of the Asp169-Glu288 pair implies that a proton is shared between the two side-chains, which, therefore, are not fully charged. Although it is impossible to assign the exact protonation state of the two groups, the existence of the Asp-Glu interaction argues against a role of Asp169 as an active-site base, possibly involved in proton abstraction from the substrate N10 atom. Rather, Asp169 seems to fulfil the role of the only H-bond acceptor for the substrate amine group. This would support the idea that the substrate is bound preferentially in the neutral form, similar to other amine oxidases/dehydrogenases such as monoamine oxidase,[17] sarcosine oxidase[18] and trimethylamine dehydrogenase.[19]

Mechanistic hypotheses

CKX reacts poorly with oxygen. This property has proven to be very useful, in that it allowed us to investigate the enzyme in the reduced form complexed to the reaction product. This, together with the complex with the slowly reacting N^6-benzyl-adenine substrate, provides a unique opportunity to visualise the enzyme in three catalytically relevant forms; the unbound native state, the form immediately before the act of oxidising the substrate (Michaelis complex) and the state right after oxidation has taken place (product complex). On this ground, a question that can be addressed is about the nature of the catalytic mechanism. For flavin-dependent amine oxidases, a "nucleophile" mechanism has been proposed by Edmondson and co-workers, with reference to human monoamine oxidases.[17] A similar mechanism has been suggested for trimethylamine dehydrogenase.[19] The mechanism envisions a nucleophilic attack by the substrate amine group onto the flavin C4a atom. This produces a covalent intermediate that leads to flavin reduction and concomitant oxidation of the

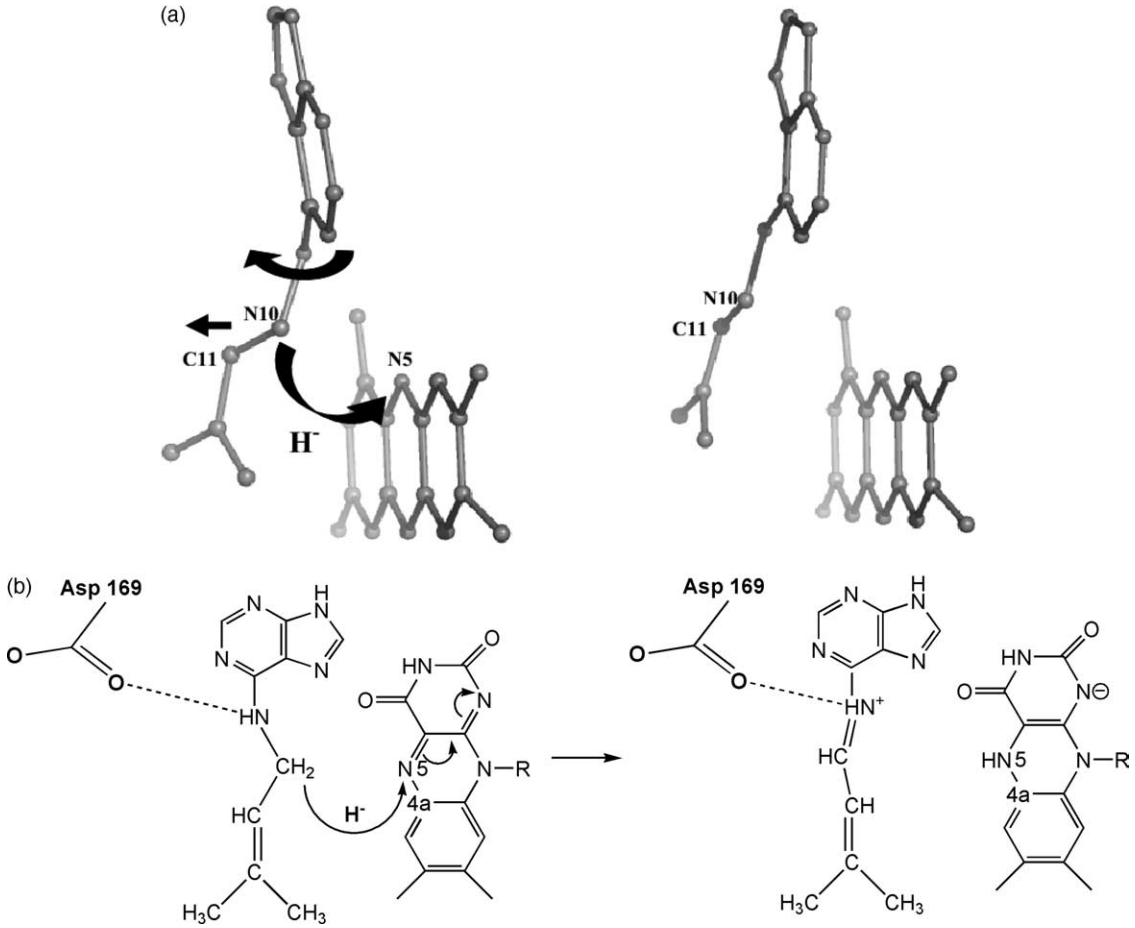

Figure 8. Structural bases of CKX catalysis. (a) The picture shows the small atomic movements expected to occur on substrate oxidation. The right-hand side picture corresponds to the experimental N^6-isopentenyladenine product complex. The left-hand side picture was generated by modelling a molecule of N^6-isopentenyladenine substrate using as reference the complex with N^6-benzyladenine. Substrate oxidation formally involves the transfer of a proton and two electrons from the substrate to the flavin (H^-). This can be brought about as direct hydride ion transfer or in a stepwise process, possibly involving radical intermediates. (b) A scheme for the substrate oxidation reaction.

substrate C–N unit. Such a mechanistic proposal has been shown to be compatible with the monoamine oxidase B crystal structure,[14] which suggests that the substrate amine group is expected to bind in front of the flavin C4a locus, positioned properly for the postulated nucleophilic attack. In CKX, however, the situation is different, because the substrate amine group points away from the flavin towards the cavity pore (Figure 7). This makes a nucleophilic attack by the substrate N10 atom on the C4a position of the cofactor stereochemically unfeasible. A feature clearly revealed by the Michaelis complex structure with N^6-benzyladenine is that the C11 carbon atom, the site of oxidative attack, points towards and is in close contact (<3.0 Å) with the flavin N5 atom. These data favour a mechanism (Figure 8) in which there is a direct transfer of the electrons and the proton to the flavin. This may involve a short-lived radical intermediate or the direct transfer of a hydride anion. In this scenario, a crucial element is represented by the Asp169 side-chain, which may polarise the substrate and favour formation of the positive charge that develops on the substrate upon oxidation (Figure 8). In this regard, CKX differs completely from monoamine oxidase[14,20] and trimethylamine dehydrogenase,[21] where the substrate amine group is recognised by an aromatic cage formed by two aromatic side-chains and the flavin ring. These observations indicate that different mechanisms for activating the substrate towards oxidation may exist: substrate polarisation through an NH…O=C H-bond in CKX and activation through a nucleophilic attack by the NH group onto the flavin C4a in monoamine oxidase and trimethylamine dehydrogenase.

In the structure of the Michaelis complex of CKX bound to N^6-benzyladenine, the C11 carbon undergoing oxidation is positioned in front of the flavin N5 with a stereochemistry (summarised in Figure 7) that closely resembles that found for the site of oxidative attack in flavin-dependent dehydrogenases and oxidases.[16] This emphasises the notion that, although the mechanism of activating the substrate towards oxidation can vary among oxidases, the precise "substrate *versus* flavin"

orientation achieved in the enzyme active site is a factor fundamental to lowering the activation energy in flavoenzyme catalysis.

Conclusions

In summary, the reaction of CKX appears to involve the following steps (Figure 8).

(1) Binding of the substrate with a plug-into-socket mode that seals the catalytic site and precisely orients the substrate C11 atom towards the reactive locus of the flavin.
(2) Stabilisation of the neutral form of the substrate amine group, which forms a H-bond to Asp169 of the Asp169-Glu288 pair.
(3) Oxidation of the substrate through formal transfer of a H^- (either stepwise or direct) from the substrate C11 to the flavin. This step may be facilitated by the stabilisation of both the developing positive charge by the N10–Asp169 H-bond interaction and the planar conformation that allows double-bond conjugation in the oxidised imine product. Substrate oxidation is coupled to a small tilt of the adenine ring inside the binding site (Figure 8(a)). One of the factors that can contribute to decrease the reactivity of N^6-benzyladenine is that the bulky benzyl ring might hinder these small but significant shifts on substrate-to-product conversion.
(4) As suggested by kinetic data, the reduced enzyme–product complex is reoxidised by an electron acceptor, followed by product release.

This last catalytic step, flavin reoxidation, poses several puzzling questions. The three-dimensional structure shows that there is no tunnel suitable for molecular oxygen transport in the active site. In addition, there is no room for an electron acceptor such as a quinone to bind in the proximity of the flavin moiety if the product has to stay bound, as indicated by the kinetic analysis (unless assuming large conformational changes, for which there is no evidence). An hypothesis could be that reoxidation could involve transfer of electrons from the flavin through the protein matrix to a quinone (or similar acceptor) bound on the surface. Verification of this hypothesis and elucidation for the mechanism for enzyme reoxidation are issues open for future studies.

Materials and Methods

Crystallisation data collection and processing

Recombinant *Zea mays* CKX was expressed in *Pichia pastoris* and purified following the published procedure.[9] The CKX crystals were obtained by the vapour-diffusion method at 293 K. The well solutions consisted of 100 mM sodium acetate (pH 4.6), 200 mM ammonium sulphate, and 12% (w/v) polyethyleneglycol 5000 monomethylether (PEG5000 MME). Sitting drops were formed by mixing equal volumes of 30 mg protein/ml in 20 mM Hepes/ KOH (pH 7.5) and well solutions. Under these conditions crystals grew after a few hours and reached a maximum size of 0.8 mm × 0.2 mm × 0.2 mm, suitable for X-ray diffraction. Binding studies were performed by soaking the crystals for one hour in solutions consisting of 150 mM sodium acetate (pH 4.6), 300 mM ammonium sulphate, and 15% (w/v) PEG5000 MME plus, respectively, 2 mM N^6-benzyladenine, 0.25 mM N^6-2-isopentenyl-adenine, and 0.5 mM *trans*-zeatin.

Before data collection, crystals were washed for a few seconds in a cryoprotectant solution consisting of 150 mM sodium acetate (pH 4.6), 300 mM ammonium sulphate, 15% (w/v) PEG5000 MME, 20% (v/v) glycerol, and ligand (when required), and then flash-cooled in a 100 K nitrogen stream. The native data used for phasing were collected using a Quantum ADSC Q4 CCD detector at ID14-EH2 beamline of the European Synchrotron Radiation Facility (Grenoble, France). The mercury derivative data were collected on a Raxis-IV imaging plate system using CuK_α radiation. Data on crystals soaked with substrates were collected on a MarCCD detector at the X13 beamline of DESY/EMBL (Hamburg, Germany), and at the X06SA beamline of SLS/PSI (Villigen, Switzerland). Crystals belong to the $P4_22_12$ space group ($a=b=171$ Å and $c=54$ Å) and contain one CKX monomer in the asymmetric unit. The X-ray data sets were processed with Mosflm[22] and scaled and reduced with programs of the CCP4 package.[23] Data collection statistics are summarised in Table 1.

Structure determination and refinement

The CKX structure was solved by single isomorphous replacement (Table 1). A heavy-atom derivative was obtained by soaking a crystal in a solution of mother liquor plus 0.1 mM $HgNO_3$ for one hour. Heavy-atoms sites were located using SHELXD.[24] Phasing and density modification was done with the program SHARP.[25]

Native data up to 1.7 Å resolution were used to automatically build most of the model by the ARP/wARP package.[26] The model was subjected to manual model building with the software package O[27] and to Refmac[28] maximum likelihood refinement. Ordered water molecules were added with the program ARP. Crystals of CKX complexes were isomorphous to those of the native enzyme. Atomic coordinates of the complexes were refined using the same protocol employed for the native structure. The same set (5% of the total) of reflections was set aside for free *R*-factor calculations during refinement of native and ligated structures.[29] The refinement statistics are summarised in Table 2.

Model analysis was carried out with DALI,[12] PROCHECK,[30] Voidoo,[31] O[27] and programs of the CCP4 package.[23] Pictures were generated with MOLSCRIPT,[32] BOBSCRIPT,[33] Raster3D,[34] Ligplot[35] and Pymol†.

Protein Data Bank accession codes

Coordinates and structure factors have been deposited in the Protein Data Bank with accession codes 1w1o, 1w1q, 1w1r, and 1w1s.

† http://www.pymol.org

Acknowledgements

We thank Dr D. E. Edmondson and W. J. H. van Berkel for advice on the manuscript. This work was supported by grants from the MIUR (COFIN03 and "Legge 449/97"), Centro Interuniversitario Biotecnologie, and Agenzia Spaziale Italiana. Data collection was performed at the Swiss Light Source (Paul Scherr Institute, Villigen, Switzerland), ESRF (Grenoble, France) and DESY/EMBL (Hamburg, Germany). We thank these synchrotron groups, whose outstanding efforts have made these experiments possible.

References

1. Mok, D. W. & Mok, M. C. (2001). Cytokinin metabolism and action. *Annu. Rev. Plant Physiol. Plant Mol. Biol.* **52**, 89–118.
2. Werner, T., Motyka, V., Strnad, M. & Schmulling, T. (2001). Regulation of plant growth by cytokinin. *Proc. Natl Acad. Sci. USA*, **98**, 10487–10492.
3. Werner, T., Motyka, V., Laucou, V., Smets, R., Van Onckelen, H. & Schmulling, T. (2003). Cytokinin-deficient transgenic Arabidopsis plants show multiple developmental alterations indicating opposite functions of cytokinins in the regulation of shoot and root meristem activity. *Plant Cell*, **15**, 2532–2550.
4. Heyl, A. & Schmulling, T. (2003). Cytokinin signal perception and transduction. *Curr. Opin. Plant Biol.* **6**, 480–488.
5. Howell, S. H., Lall, S. & Che, P. (2003). Cytokinins and shoot development. *Trends Plant Sci.* **8**, 453–459.
6. Schmulling, T., Werner, T., Riefler, M., Krupkova, E. & Bartrina y Manns, I. (2003). Structure and function of cytokinin oxidase/dehydrogenase genes of maize, rice, Arabidopsis and other species. *J. Plant Res.* **116**, 241–252.
7. Fraaije, M. W., Benen, J. A. E., Visser, J., van Berkel, W. J. H. & Mattevi, A. (1998). A novel oxidoreductase family sharing a conserved FAD-binding domain. *Trends Biochem. Sci.* **23**, 206–207.
8. Galuszka, P., Frebort, I., Sebela, M., Sauer, P., Jacobsen, S. & Pec, P. (2001). Cytokinin oxidase or dehydrogenase? Mechanism of cytokinin degradation in cereals. *Eur. J. Biochem.* **268**, 450–461.
9. Bilyeu, K. D., Cole, J. L., Laskey, J. G., Riekhof, W. R., Esparza, T. J., Kramer, M. D. & Morris, R. O. (2001). Molecular and biochemical characterization of a cytokinin oxidase from maize. *Plant Physiol.* **125**, 378–386.
10. Frébortová, J., Fraaije, M. W., Galuszka, P., Sebela, M., Pec, P., Hrbac, J. *et al.* (2004). Catalytic reaction of cytokinin dehydrogenase: preference for quinones as electron acceptors. *Biochem. J.* **380**, 121–131.
11. Morris, R. O., Bilyeu, K. D., Laskey, J. G. & Cheikh, N. N. (1999). Isolation of a gene encoding a glycosylated cytokinin oxidase from maize. *Biochem. Biophys. Res. Commun.* **255**, 328–333.
12. Holm, L. & Sander, C. (1993). Protein structure comparison by alignment of distance matrices. *J. Mol. Biol.* **233**, 123–138.
13. Coulombe, R., Yue, K. Q., Ghisla, S. & Vrielink, A. (2001). Oxygen access to the active site of cholesterol oxidase through a narrow channel is gated by an Arg-Glu pair. *J. Biol. Chem.* **276**, 30435–30441.
14. Binda, C., Li, M., Hubálek, F., Restelli, N., Edmondson, D. E. & Mattevi, A. (2003). New insights into the mode of inhibition of human mitochondrial monoamine oxidase B from high resolution crystal structures. *Proc. Natl Acad. Sci. USA*, **100**, 9750–9755.
15. Fraaije, M. W., van den Heuvel, R. H. H., van Berkel, W. J. H. & Mattevi, A. (1999). Covalent flavinylation is essential for efficient redox catalysis in vanillyl-alcohol oxidase. *J. Biol. Chem.* **274**, 35514–35520.
16. Fraaije, M. W. & Mattevi, A. (2000). Flavoenzymes: diverse catalysts with recurrent features. *Trends Biochem. Sci.* **25**, 126–132.
17. Miller, J. R. & Edmondson, D. E. (1999). Structure–activity relationships in the oxidation of para-substituted benzylamine analogues by recombinant human liver monoamine oxidase A. *Biochemistry*, **38**, 13670–13683.
18. Zhao, G. & Jorns, M. S. (2002). Monomeric sarcosine oxidase: evidence for an ionizable group in the E.S complex. *Biochemistry*, **41**, 9747–9750.
19. Basran, J., Sutcliffe, M. J. & Scrutton, N. S. (2001). Optimising the Michaelis complex of trimethylamine dehydrogenase: identification of interactions that perturb the ionization of substrate and facilitate catalysis with trimethylamine base. *J. Biol. Chem.* **276**, 42887–42892.
20. Binda, C., Mattevi, A. & Edmondson, D. E. (2002). Structure–function relationships in flavoenzyme-dependent amine oxidations. A comparison of polyamine oxidase and monoamine oxidase. *J. Biol. Chem.* **277**, 23973–23976.
21. Trickey, P., Basran, J., Lian, L. Y., Chen, Z., Barton, J. D., Sutcliffe, M. J. *et al.* (2000). Structural and biochemical characterisation of recombinant wild type and a C30A mutant of trimethylamine dehydrogenase from *Methylophilus methylotrophus* (sp. W(3)A(1)). *Biochemistry*, **39**, 7678–7688.
22. Leslie, A. G. (1999). Intregration of macromolecular diffraction data. *Acta Crystallog. sect. D*, **55**, 1696–1702.
23. Collaborative Computational Project Number 4. (1994). The CCP4 suite: programs for protein crystallography. *Acta Crystallog. sect. D*, **50**, 760–767.
24. Schneider, T. R. & Sheldrick, G. M. (2002). Substructure solution with SHELXD. *Acta Crystallog. sect. D*, **58**, 1772–1779.
25. Bricogne, G., Vonrhein, C., Flensburg, C., Schiltz, M. & Paciorek, W. (2003). Generation, representation and flow of phase information in structure determination: recent developments in and around SHARP 2.0. *Acta Crystallog. sect. D*, **59**, 2023–2030.
26. Perrakis, A., Morris, R. J. & Lamzin, V. S. (1999). Automated protein model building combined with iterative structure refinement. *Nature Struct. Biol.* **6**, 458–463.
27. Jones, T. A., Zou, J. Y., Cowan, S. W. & Kjeldgaard, M. (1991). Improved methods for building protein models in electron density maps and the location of errors in these models. *Acta Crystallog. sect. A*, **47**, 110–119.
28. Murshudov, G. N., Vagin, A. A. & Dodson, E. J. (1997). Refinement of macromolecular structures by the maximum-likelihood method. *Acta Crystallog. sect. D*, **53**, 240–255.
29. Brunger, A. T. (1992). The free R value. A novel statistical quantity for assessing the accuracy of crystal structures. *Nature*, **355**, 472–475.
30. Laskowski, R. A., MacArthur, M. W., Moss, D. S. &

Thornton, J. M. (1993). PROCHECK: a program to check the stereochemistry quality of protein structures. *J. Appl. Crystallog.* **26**, 283–291.
31. Kleywegt, G. J. & Jones, T. A. (1994). Detection, delineation, measurement and display of cavities in macromolecular structures. *Acta Crystallog. sect. D*, **50**, 178–185.
32. Kraulis, P. J. (1991). MOLSCRIPT: a program to produce both detailed and schematic plots of protein structures. *J. Appl. Crystallog.* **24**, 946–950.
33. Esnouf, R. M. (1999). Further additions to MolScript version 1.4, including reading and contouring of electron-density maps. *Acta Crystallog. sect. D*, **55**, 938–940.
34. Merritt, E. A. & Bacon, D. J. (1997). Raster3D: photorealistic molecular graphics. *Methods Enzymol.* **277**, 505–524.
35. Wallace, A. C., Laskowski, R. A. & Thornton, J. M. (1995). LIGPLOT: a program to generate schematic diagrams of protein–ligand interactions. *Protein Eng.* **8**, 127–134.

Edited by R. Huber

(Received 31 March 2004; received in revised form 21 June 2004; accepted 23 June 2004)